

Micro-Raman and cathodoluminescence studies of epitaxial laterally overgrown GaN with tungsten masks: A method to map the free-carrier concentration of thick GaN samples

A. Kaschner,^{a)} A. Hoffmann, and C. Thomsen

Institut für Festkörperphysik, Technische Universität Berlin, Hardenbergstraße 36, 10623 Berlin, Germany

F. Bertram, T. Riemann, and J. Christen

Institut für Experimentelle Physik, Otto-von-Guericke-Universität, P. O. Box 4120, 39016 Magdeburg, Germany

K. Hiramatsu

Department of Electrical and Electronic Engineering, Faculty of Engineering, Mie University, 1515 Kamihama-cho, Tsu, Mie 514-8507, Japan

H. Sone and N. Sawaki

Department of Electronics, School of Engineering, Nagoya University, Furo-cho, Chikusa-ku, Nagoya, Aichi 464-8603, Japan

(Received 21 October 1999; accepted for publication 12 April 2000)

Cathodoluminescence (CL) and micro-Raman spectroscopy were applied to study microscopically the optical and structural properties of two epitaxial-laterally overgrown GaN structures with tungsten masks in $\langle 1\bar{1}00 \rangle$ and $\langle 11\bar{2}0 \rangle$ direction, respectively. A free-carrier concentration higher than 10^{19} cm^{-3} was observed right above the masks, leading to a gradient in free-carrier concentration over the whole layer thickness. We used the normalized longitudinal-optical-phonon intensity and the broad band around 650 cm^{-1} as a measure for the free-electron concentration, which is a promising method to determine the free-carrier concentration justified by the good correlation with CL results. © 2000 American Institute of Physics. [S0003-6951(00)00823-8]

The importance of epitaxial laterally overgrown GaN (ELOG) as a substrate for the production of laser diodes in the ultraviolet spectral range with lifetimes of some 1000 h was pointed out by Nakamura *et al.*¹ The main effect is the reduction of the threading dislocation density from 10^{10} to 10^6 cm^{-2} in the overgrown region, although the physical consequences of this fact are not yet completely understood. Chichibu *et al.*² showed that the recombination dynamics in InGaN quantum wells on ELOG substrate is not affected by the dislocation density. Other efforts in the field of growth and characterization of overgrown GaN include the replacement of the SiO_2 masks by tungsten masks³ to prevent the in-diffusion of silicon and oxygen atoms in the overgrown GaN, which was suggested to be the origin of the high free-carrier concentration above the masks.^{4,5} A new method called pendeoepitaxy has been established to achieve a more uniformly low density of defects in the material.⁶

In this letter, we report on μ -Raman and cathodoluminescence (CL) studies of two ELOG samples with tungsten masks. The samples investigated here consist of a 4- μm -thick GaN layer grown by metal-organic vapor phase epitaxy (MOVPE) on a (0001) sapphire substrate patterned with a 50-nm-thick tungsten mask. The parallel mask stripes are oriented along the $\langle 1\bar{1}00 \rangle \langle 11\bar{2}0 \rangle$ direction for sample A(B). The width of the openings and the stripes are 10 μm and 5 μm sample A(B). This structure was subsequently overgrown with an approximately 35- μm -thick GaN layer deposited by hydride vapor phase epitaxy (HVPE).³ The samples were cleaved resulting in a smooth cross section area. The

room-temperature μ -Raman measurements ($\lambda=488 \text{ nm}$) were carried out in backscattering geometry perpendicular to the c -axis.⁵ The spatial and energetic resolution was 0.7 μm and 0.1 cm^{-1} , respectively. The CL measurements were performed similarly as described in Refs. 4 and 5.

Figure 1(a) shows a secondary electron image of the cross section of sample A. The sample surface, as well as for

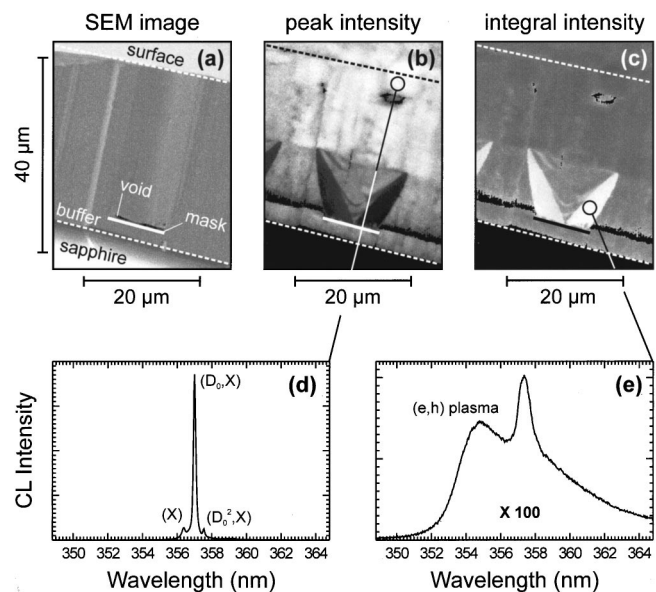


FIG. 1. SEM image (a), CL peak intensity ratio $I_{\text{peak}}/I_{\text{int}}$ (b), and integral CL intensity ratio $I_{\text{int}}/I_{\text{peak}}$ (c) mappings of the sample cross section of an ELOG sample with tungsten masks parallel to $\langle 1\bar{1}00 \rangle$ direction measured under 45° observation angle. Locally averaged CL spectra from the upper half of the ELO layer (d) and from the bunny-ear-like structures (e) are depicted for comparison.

^{a)}Electronic mail: kaschner@physik.tu-berlin.de

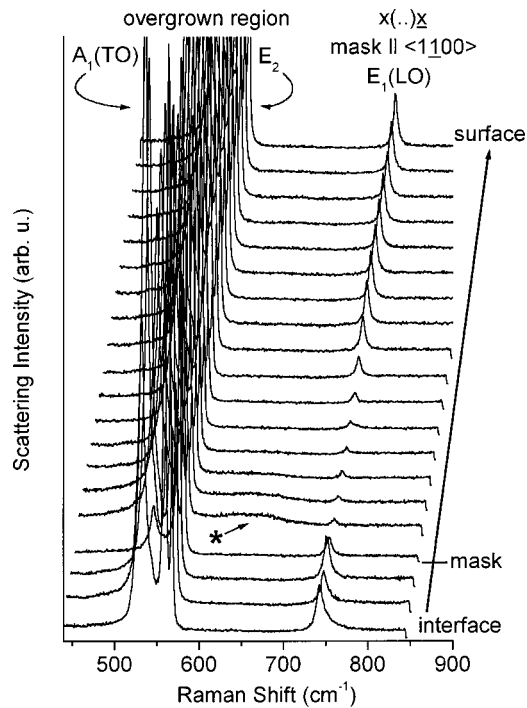


FIG. 2. Room-temperature Raman spectra taken at various distances from the substrate interface in the overgrown region. The disappearance of the LO mode and the appearance of the mode at around 650 cm^{-1} (marked by an asterisk) is a measure for the free-carrier concentration.

sample B (not shown), exhibits a smooth surface. This is different to the ELOG structures with SiO_2 masks, where the sample with the stripes parallel to $\langle 1\bar{1}00 \rangle$ direction showed small dips at the surface above the masks.⁵ This was even more pronounced for the sample with the SiO_2 masks in $\langle 11\bar{2}0 \rangle$ direction which resulted in a roof-like surface morphology.⁴ Also it can be seen in the SEM image, that the use of tungsten masks leads to voids on top of the masks with a flat pyramid-like shape up to $1\ \mu\text{m}$ in height.

In Fig. 1(b) we show a CL mapping of the ratio $I_{\text{peak}}/I_{\text{int}}$ and the reciprocal mapping of $I_{\text{int}}/I_{\text{peak}}$ is plotted in Fig. 1(c). The dramatic changes of the spectral properties in the different growth domains are obvious. Above the mask bunny-ear-shaped regions of a broad luminescence [dark in Fig. 1(b); bright in Fig. 1(c)] at the edge of the lateral growth region³ appear indicating a strong enhancement of the local free carrier concentration due to defects. This is directly evidenced by the local CL spectrum Fig. 1(e) averaged over both ‘‘bunny-ears.’’ This CL spectrum is dominated by an extremely broad blue-shifted emission band originating from $e-h$ plasma recombination.

Half way from the interface to the surface the luminescence becomes excitonic over the whole lateral extension with slightly fluctuating line positions. This is visualized by the bright contrast in Fig. 1(b). Right below the surface a sharp excitonic luminescence at 357 nm is found indicating the high crystalline quality of the material as well as the low local free carrier concentration [see Fig. 1(d)].

We performed μ -Raman experiments to determine the free-carrier concentration by the position of the coupled phonon-plasmon modes in the spectra. It turned out that neither LPP^+ modes with frequencies higher than the E_1 longitudinal-optical (LO) mode nor LPP^- modes could be

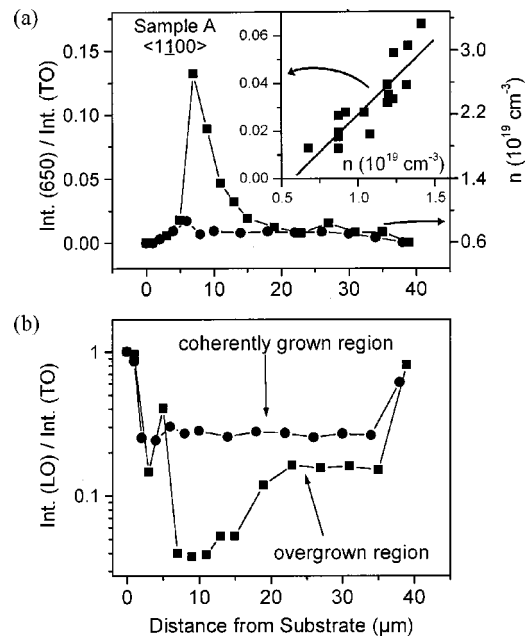


FIG. 3. Normalized intensity of the LO mode (b) and the 650 cm^{-1} structure (a) as a function of the distance from the substrate interface for both regions of sample A. The inset of (a) shows the intensity of the 650 cm^{-1} mode vs free-carrier concentration derived from the data in Refs. 4 and 5.

detected. This is probably due to an overdamping of the excitations of the free-electron gas.^{7,8} For high values of the plasmon damping the LPP modes are strongly broadened and not observable. However, we found two strong indications that there is a high free-carrier concentration in some regions as suspected from the CL results. In Fig. 2 μ -Raman spectra at different distances from the substrate interface are plotted for the overgrown (mask) region of sample A. In the $x(\dots)x$ scattering geometry the A_1 transverse-optical (TO), $E_1(\text{TO})$, E_2 (high, low) and the Fröhlich-allowed $E_1(\text{LO})$ mode are observed.⁹ One can clearly see a disappearance of the $E_1(\text{LO})$ mode in the region above the tungsten mask accompanied by the appearance of a broad structure around 650 cm^{-1} . Careful inspection shows only a slight variation of the LO-mode intensity at different points in the coherently grown region. According to Ref. 8 a relaxation of the \mathbf{q} conservation due to defects can give rise to a continuous scattering in the TO–LO range which is determined by the density of LO phonon states interacting with free carriers. Furthermore it was shown for cubic n -type GaN that nonconservation of \mathbf{q} in over-damped electron plasmas may lead to a broad plasmon-related structure in the region between TO and LO mode.¹⁰ Therefore we think that the 650 cm^{-1} structure appearing in certain spectra of our samples is plasmon-related and thus related to the free-electron concentration. Figure 3(a) shows the intensity of the 650 cm^{-1} structure normalized to the $A_1(\text{TO})$ intensity. The integral intensity was determined between 590 and 720 cm^{-1} after linear background subtraction. From our previous data^{4,5} we found a linear relation between the normalized intensity of the 650 cm^{-1} band and the free-carrier concentration between 6×10^{18} and $1.5 \times 10^{19}\text{ cm}^{-3}$ [see inset of Fig. 3(a)]:

$$\frac{\text{Int.}(650)}{\text{Int.}[A_1(\text{TO})]} = (-0.04 \pm 0.01) + (6 \pm 1) 10^{-21} n (\text{cm}^{-3}). \quad (1)$$

Figure 3(b) shows the normalized $E_1(\text{LO})$ intensity where

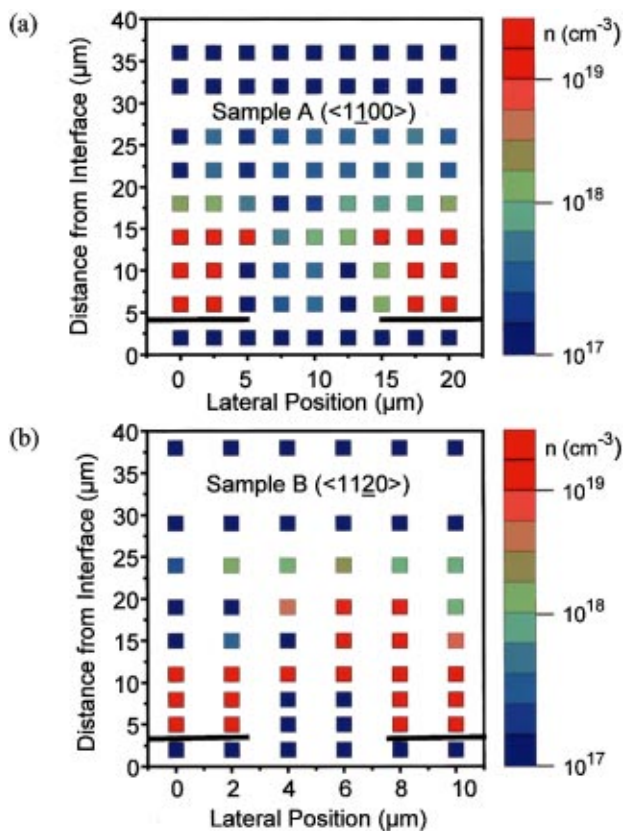


FIG. 4. (Color) Mapping of the local free-carrier concentration of sample A (a) and B (b) in vertical and lateral direction. Black bars indicate the position of the tungsten masks. The color scale gives the order of magnitude of the free-carrier concentration.

the maximum was set to be unity for both the mask and the window region. We observe a maximum intensity for the 650 cm^{-1} structure $7\text{ }\mu\text{m}$ away from the substrate interface, i.e., right above the void, coinciding with a minimum LO intensity at the same distance. A strong gradient in the LO intensity is found in the overgrown region with a complete recovering at the sample surface. In contrast, in the coherently grown region the value for the normalized LO intensity stays almost constant between 2 and $34\text{ }\mu\text{m}$.

In the following we used this procedure to map the local free-carrier concentration also in lateral direction. In Fig. 4 such a mapping is shown for both sample A (a) and B (b). The color of the squares at each sampling point indicates the free-carrier concentration. The scaling was done with the described procedure using the normalized intensity of the 650 cm^{-1} band and the LO mode. In sample regions where the 650 cm^{-1} band was not found but the $E_1(\text{LO})$ mode with maximum intensity, i.e., in the MOVPE-GaN layer, the free-carrier concentration was estimated to be 10^{17} cm^{-3} . Our method gives a rough measure accurate to one order of magnitude. For sample A we find a highly defective region right in the middle above the masks, i.e., in the coalescence region. The free-carrier concentration decreases in vertical direction. Note that the region with a high free-carrier concentration (red and green squares) broadens up to a distance of $18\text{ }\mu\text{m}$ from the interface. This directly mirrors the lateral growth region (compare with Fig. 2 in Ref. 3) and coincides with the bunny-ear-shaped structure in the CL images [Figs. 1(b) and 1(c)]. At $22\text{ }\mu\text{m}$ from the interface the carrier con-

centration is slightly less than 10^{18} cm^{-3} at any lateral position, further decreasing and reaching 10^{17} cm^{-3} right below the surface. In this region no lateral growth occurs, but growth in vertical (c -) direction. A similar behavior is found for sample B having the stripes in $\langle 11\bar{2}0 \rangle$ direction, but two differences are obvious. First, at $24\text{ }\mu\text{m}$ from the interface the free-carrier concentrations are clearly higher than the 10^{18} cm^{-3} at $22\text{ }\mu\text{m}$ for sample A. This suggests that the extension of the defective region or the in-diffusion of free carriers proceeds somewhat further for sample B. Second, the highly defective regions merge together at $12\text{ }\mu\text{m}$ (only red squares in a line) from the interface for sample B, whereas they are clearly separated in sample A. This is a result of the $10\text{ }\mu\text{m}$ mask pattern period for sample B compared with the $20\text{ }\mu\text{m}$ period of sample A.

We investigated two ELOG samples with tungsten masks parallel to $\langle 1\bar{1}00 \rangle$ and $\langle 11\bar{2}0 \rangle$ direction using μ -Raman spectroscopy to determine the local free-carrier concentration. Because of the absence of LPP modes we determined the free-carrier concentration from the normalized intensity of the 650 cm^{-1} band and the $E_1(\text{LO})$ mode, which is in the present scattering configuration due to Fröhlich interaction.

As a result we find a highly defective region above the masks which broadens with increasing distance from the interface. This nicely coincides with the growth model³ where a lateral growth region with the shape of an inverted triangle was predicted and agrees with the CL images. The differences between the two samples can be explained mainly by their different mask pattern periods.

Due to the high melting point of tungsten in-diffused mask atoms can be excluded as the origin of the high free-carrier concentration above the masks. Intrinsic defects or dopant atoms from the growth atmosphere accumulating in the region above the masks are much more probable.

A. Kaschner acknowledges the support of an Ernst-von-Siemens-scholarship. Part of this work was supported by the Deutsche Forschungsgemeinschaft (DFG).

¹S. Nakamura, M. Senoh, S. Nagahama, N. Iwasa, T. Yamada, T. Matsushita, H. Kiyoku, Y. Sugimoto, T. Kozaki, H. Umemoto, M. Sano, and K. Chocho, Appl. Phys. Lett. **72**, 211 (1998).

²S. F. Chichibu, H. Marchand, M. S. Minsky, S. Keller, P. T. Fini, J. P. Ibbetson, S. B. Fleischer, J. S. Speck, J. E. Bowers, E. Hu, U. K. Mishra, S. P. DenBaars, T. Deguchi, T. Sota, and S. Nakamura, Appl. Phys. Lett. **74**, 1460 (1999).

³H. Sone, S. Nambu, Y. Kawaguchi, M. Yamaguchi, H. Miyake, K. Hiramatsu, Y. Iyechika, T. Maeda, and N. Sawaki, Jpn. J. Appl. Phys., Part 2 **38**, L356 (1999).

⁴F. Bertram, T. Riemann, J. Christen, A. Kaschner, A. Hoffmann, C. Thomsen, K. Hiramatsu, T. Shibata, and N. Sawaki, Appl. Phys. Lett. **74**, 359 (1999).

⁵A. Kaschner, A. Hoffmann, C. Thomsen, F. Bertram, T. Riemann, J. Christen, K. Hiramatsu, T. Shibata, and N. Sawaki, Appl. Phys. Lett. **74**, 3320 (1999).

⁶K. Linthicum, T. Gehrke, D. Thomson, E. Carlson, P. Rajagopal, T. Smith, D. Batchelor, and R. F. Davis, Appl. Phys. Lett. **75**, 196 (1999).

⁷T. Kozawa, T. Kachi, H. Kano, Y. Taga, M. Hashimoto, N. Koide, and K. Manabe, J. Appl. Phys. **75**, 1098 (1994).

⁸F. Demangeot, J. Frandon, M. A. Renucci, C. Meny, O. Briot, and R. L. Aloumbard, J. Appl. Phys. **82**, 1305 (1997).

⁹H. Siegle, L. Eeckey, A. Hoffmann, C. Thomsen, B. K. Meyer, D. Schikora, M. Hankeln, and K. Lischka, Solid State Commun. **96**, 943 (1995).

¹⁰M. Ramsteiner, O. Brandt, and K. H. Ploog, Phys. Rev. B **58**, 1118 (1998).